

Translocation frequency of double-stranded DNA through a solid-state nanopore

Nicholas A. W. Bell¹, Murugappan Muthukumar^{1,2}, and Ulrich F. Keyser¹

¹*Cavendish Laboratory, University of Cambridge, CB3 0HE, UK and*

²*Polymer Science and Engineering Department, University of Massachusetts, Amherst, Massachusetts 01003, USA*

Solid-state nanopores are single molecule sensors that measure changes in ionic current as charged polymers such as DNA pass through. Here, we present comprehensive experiments on the length, voltage and salt dependence of the frequency of double-stranded DNA translocations through conical quartz nanopores with mean opening diameter 15 nm. We observe an entropic barrier limited, length dependent translocation frequency at 4M LiCl salt concentration and a drift-dominated, length independent translocation frequency at 1M KCl salt concentration. These observations are described by a unifying convection-diffusion equation which includes the contribution of an entropic barrier for polymer entry.

Polymer translocation through a narrow pore is a ubiquitous process in organisms. Classic examples include the passage of mRNA across the nuclear pore complex and DNA ejection by a bacteriophage. *In vitro* experiments on polymer translocation are possible using nanopores fabricated in solid-state materials or with reconstituted membrane proteins. The basic method for sensing the translocation of a polymer, such as DNA, relies on applying a voltage across the nanopore and measuring changes in ionic current as molecules pass through. This simple premise underlies research for developing nanopores as biosensors for instance in next-generation sequencing applications [1]. Yet experimental data on polymer translocation phenomena present many puzzles that remain to be fully understood [2].

Conceptually, the electrophoretically driven translocation of DNA through a nanopore consists of essentially three steps; (i) the DNA moves towards the pore entrance by a combination of diffusion and drift due to the electric field outside the pore, (ii) the DNA is captured at the mouth of the pore, and (iii) the DNA threads through the nanopore causing a detectable ionic current change. All three steps taken together determine the translocation frequency defined here as the number of DNA strands passing through the nanopore per second per unit concentration. Accurate measurements of the translocation frequency enable characterisation of the transport process and are important for applications in nucleic acid sensing.

For the α -hemolysin nanopore, the translocation frequency of short, single-stranded (ss)DNA shows an exponential dependence on voltage under typical experimental conditions indicating a barrier-limited process [3–5]. At high voltages and polymer concentrations, a second exponential is observed which is attributed to the effect of polymer-polymer interactions at the pore mouth [4]. Small diameter (sub 5-nm) solid-state nanopores show an increasing translocation frequency with double-stranded (ds)DNA length from 0.4 kbp to ~ 8 kbp followed by an indication of a length independent translocation frequency for longer lengths [6]. Electro-osmotic flow effects on the dsDNA trapped at the membrane surface were suggested as a reason for the length dependence

of translocation frequency [6, 7]. It is known that the small diameter of these nanopores relative to the dsDNA cross-section results in strong interactions between the dsDNA and pore surface [8, 9]. Larger nanopores, with diameters several times the cross section of dsDNA, show significantly less spread in transit times due to the lack of strong surface interactions [8]. This enables a simpler physical picture with the translocation speed accurately modelled by a combination of hydrodynamics and continuum electrostatics [10, 11]. While many reports in the literature have characterised the threading speed and conformations of dsDNA in these wide nanopores [12–14] there are few measurements on the translocation frequency which can provide insight on the underlying transport mechanisms.

In this paper, towards developing a complete picture of dsDNA translocation in solid-state nanopores, we study the voltage, length, salt and concentration dependence of dsDNA translocation frequency for nanopores with diameters 15 ± 3 nm. We show the simultaneous detection of ten different DNA lengths in the range 0.5 kbp to 10 kbp which allows us to accurately characterize the translocation frequency. In 4M LiCl electrolyte, there is an increase in translocation frequency with DNA length whereas experiments using 1M KCl show a length independent translocation frequency. These trends are accurately captured by a 1D convection-diffusion equation which incorporates an entropic barrier for polymer entry into the nanopore and scaling laws for polymer diffusion and mobility.

Quartz capillaries were fabricated into nanopores using a previously published protocol with diameters 15 ± 3 nm (mean \pm s.d.) [15]. The nanopore was filled with a solution of 10 mM Tris-HCl pH 8, 1 mM EDTA and electrolyte (either 4M LiCl or 1M KCl). DNA was added to the reservoir containing the nanopore tip which was set as the electrical ground. Fig. 1a shows a typical scanning electron microscope image of a conical quartz nanopore and in Fig. 1b the electric field profile at +600 mV applied potential is shown from finite-element calculations. The electric field was calculated using a finite-element solver (COMSOL 4.4) and the full Poisson-Nernst-Planck equations for ion transport through the pore in a 2D ax-

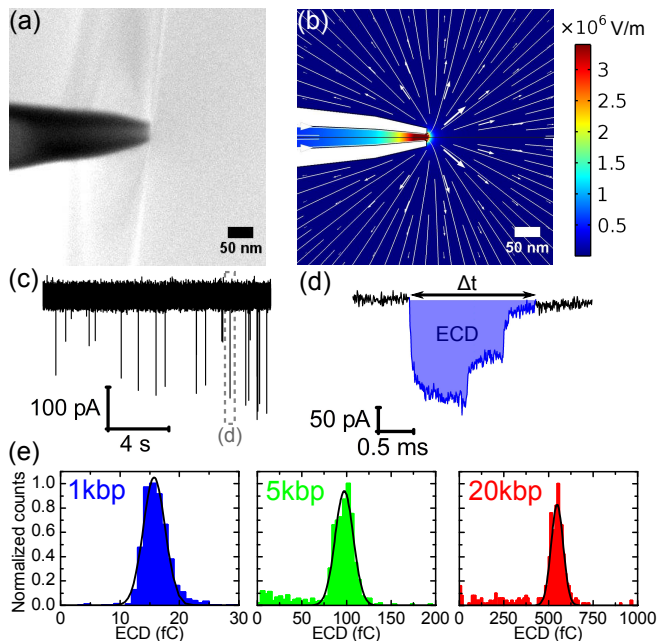


FIG. 1. (a) Scanning electron microscope image of a typical quartz nanopore. (b) Finite-element analysis of the electric field profile at a voltage of +600 mV using the geometric model given in [15]. Lines represent tangents to the electric field. (c) Typical current trace showing downward spikes due to DNA translocation interrupting the baseline. The event in the dashed area is shown at greater time resolution in (d) which also shows the event charge deficit (ECD) in blue - the integrated area of the event relative to the baseline. (e) Histograms of ECD for 1 kbp, 5 kbp and 20 kbp DNA with $N=1119$, $N=764$ and $N=456$ translocations respectively. Each length was measured separately at +600 mV with a DNA concentration of 1.6 nM.

isymmetric geometry. The electric field is mainly confined to the last few hundred nanometres of the tip and decays rapidly away from the pore entrance. Ionic currents were measured using an Axopatch 200B amplifier, filtered at 50 kHz using an external 8-pole Bessel filter and subsequently sampled at 250 kHz. All data was analysed with a custom-written program in Labview 2013 (National Instruments). All experiments were performed at 20°C. Translocations were detected using a threshold analysis with minimum current change set to 50 pA, minimum translocation duration 50 μ s and minimum event charge deficit of 3 fC. The translocations from all DNA lengths at all voltages fall outside these limits and therefore we do not miss translocations.

Initially we characterised the translocation of individual dsDNA lengths in 4M LiCl electrolyte. We observe that dsDNA can translocate in folded configurations in agreement with previous studies using similar sized nanopores [13, 16]. This is shown by the quantised levels of current blockade as for example in Fig. 1d. For 10 kbp DNA we observe folded configurations with up to three double-strands of the same molecule in the pore. The translocation time is determined by both the DNA

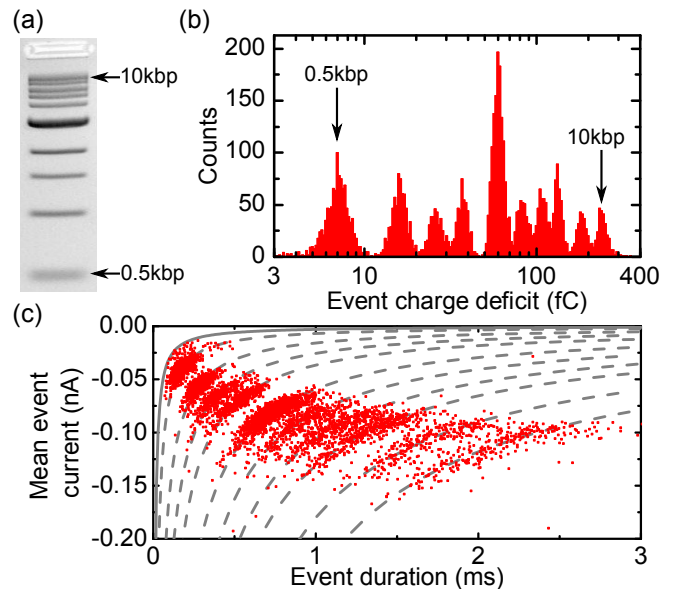


FIG. 2. (a) Agarose gel (1%) electrophoretogram of the DNA sample containing 10 lengths in the range 0.5 kbp to 10 kbp. (b) ECD histogram for 5711 translocation events recorded at +600 mV. The histogram is logarithmically binned and the peaks corresponding to the shortest and longest DNA lengths are labelled. (c) Scatter plot of mean event current against event duration for same events as in (b). The dashed grey lines are fits according to $\Delta I_{Mean} = -\frac{ECD_{Peak}}{\Delta t}$ and the solid line shows the 3 fC threshold.

length and the folding configuration of the DNA and does not uniquely identify a *single* DNA length. However, the integral of the current with respect to time or event charge deficit (ECD), can be used to distinguish each DNA length. Fig. 1e shows ECD distributions of individual dsDNA lengths of 1 kbp, 5 kbp and 20 kbp which are single peaks each well fitted by a Gaussian function (Fig. 1e). Outliers are observed at low ECD values for both 5 kbp and 20 kbp which we attribute to a small amount of fragmentation from DNA shearing which can occur during pipetting of long DNA molecules [17] and has been observed previously [12].

Our observation of a single peak in ECD for each DNA length strongly suggests that we only measure a current signal above the background noise when the molecule fully translocates through the nanopore. It is also possible that there are events where the DNA is captured at the pore mouth but does not overcome the energy barrier to translocation and therefore returns to the sample reservoir under thermal motion. These collisions can create a second population and have been observed for dsDNA in sub-5 nm solid-state nanopores [8, 9] and for ssDNA in α -hemolysin [18]. We attribute the lack of a second population from collisions as being due to the conical shape of the nanopores meaning that the effective sensing length is on the order of a few hundred nanometres. Therefore collisions do not cause a significant enough current change to be measured above the noise.

For accurate, simultaneous determination of translocation frequency of a range of lengths, we used a mixture of 10 DNA lengths in the range 0.5 kbp to 10 kbp (Fig. 2a). The ECD histogram for 5711 translocations with 4M LiCl electrolyte is shown in Fig. 2b and Fig. 2c shows the corresponding scatter plot of mean current versus duration for each translocation. The low noise of quartz nanopores combined with the slow DNA velocity in 4M LiCl means that we have sufficient resolution to identify the 10 DNA lengths present with each DNA length in the scatter plot observed as a band. The dashed grey lines are given by $\Delta I_{Mean} = -\frac{ECD_{Peak}}{\Delta t}$ where ΔI_{Mean} is the mean event current, Δt is the event duration and ECD_{Peak} is the centre of the Gaussian function determined by fitting each ECD peak. The excellent fit of this equation to the data confirms that for all translocations of a particular length, the ECD value is constant irrespective of the folding state of the DNA as it passed through. As described earlier, we assign each data point to a translocation of DNA and therefore determined the total number of translocations for each length from the integrated area of Gaussian functions fitted to each peak in the ECD histogram. The translocation frequency (shown in Fig. 4) was then calculated as $N/c\tau$ where N is the number of translocations, c is the DNA concentration and τ is the experiment time.

We use the following model to describe the DNA translocation frequency based on Muthukumar [19]. Our general strategy is to model a stochastic one-dimensional process of the polymer negotiating a free-energy landscape using known bulk solution scaling laws for the diffusion coefficient and electrophoretic mobility. The 15 nm mean diameter of the nanopores used in this study is significantly bigger than the 2 nm diameter of dsDNA. Therefore we assume that the main free-energy barrier for translocation is entropic in nature due to the restriction of the number of conformations of a translocating DNA molecule. The net flux of molecules is determined by this entropic barrier, diffusion of the DNA and the electrophoretic force acting on the DNA. We can neglect electro-osmotic flows since measurements using optical tweezers show that the flow rate decreases strongly with salt concentration and is insignificant compared to the electrophoretic force at the high salt concentrations used here [20, 21].

The flux, $J(x, t)$, is therefore given by a 1D convection-diffusion equation:

$$J(x, t) = -D \frac{\partial c(x, t)}{\partial x} - c(x, t) \mu \frac{\partial V(x)}{\partial x} - \frac{Dc(x, t)}{kT} \frac{\partial F(x)}{\partial x}, \quad (1)$$

where D is the diffusion coefficient, x is the centre of mass coordinate of the DNA, $c(x, t)$ is the concentration, μ is the electrophoretic mobility, $V(x)$ is the electric potential, T is the temperature and $F(x)$ is the entropic barrier. We model the nanopore geometry as cylindrical with length L and the entropic barrier as triangular

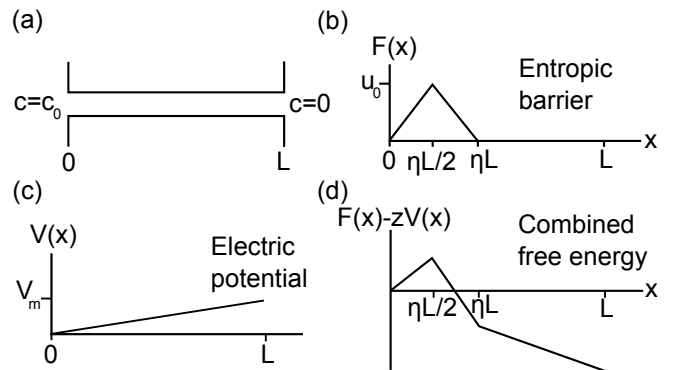


FIG. 3. (a) Modelled 1D geometry for the nanopore with length L , concentration c_0 in the sample reservoir and zero in the opposing reservoir. (b) Triangular profile for the entropic barrier $F(x)$ with height u_0 . η parameterises how far the barrier extends into the pore. (c) The electric potential (V_m is the applied voltage) and (d) combined free energy profile for the nanopore where z is the effective DNA charge.

with height u_0 at a distance $\eta L/2$ from the pore mouth (Fig. 3). η therefore describes the distance the entropic barrier extends into the nanopore. We estimated $\eta=0.25$ based on assuming that the entropic barrier extends 50 nm (approximately one persistence length of dsDNA) and assuming a pore length of 200 nm. The concentration is c_0 at the entrance and zero at the exit. The electric field contribution in front of the pore mouth is neglected since it rapidly decays (Fig. 1b).

For single file DNA threading through a nanopore, theoretical calculations suggest a weak $N^{-0.2}$ dependence of barrier height u_0 on DNA length N [22]. However, the nanopore diameter used here allows for non-single file threading for which the length dependence of the entropic barrier has not been calculated and we assume a barrier height independent of the DNA length. Naturally, a more complicated profile for the nanopore geometry and entropic barrier can be used but we choose this one since our goal is to capture the essential physics of the transport process and our chosen profile is readily solved analytically.

By applying steady-state boundary conditions, we calculate the translocation frequency as the flux at the pore exit from equation (1). We assume the diffusion coefficient and electrophoretic mobility scale with length according to relationships observed in bulk solution. The diffusion coefficient, D , of dsDNA in the length regime 0.5 kbp to 10 kbp scales with the chain length as $D \sim N^{-0.6}$ [23, 24]. It is also known that electrophoretic mobility is independent of N , $\mu \sim N^0$ [25]. These dependencies are included in the calculations and give the length dependence for the translocation frequency.

Fig. 4a shows our experimental data for the length dependence of translocation frequency in 4M LiCl. We observe that the translocation frequency increases with increasing DNA length with an offset and steepness determined by the applied voltage. The trend lines shown

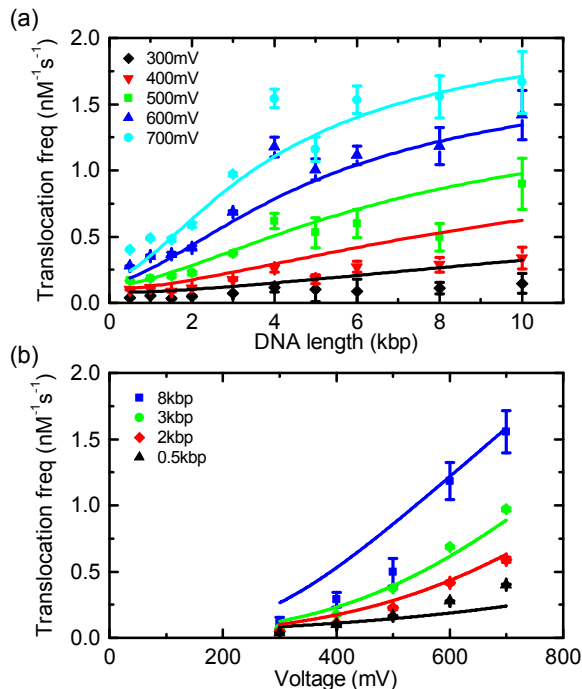


FIG. 4. (a) Length dependence of DNA translocation frequency measured at five different voltages (all data from the same nanopore) in an electrolyte of 4M LiCl. The trend lines show least-squares fits to the data using equation (2) and the model of Fig. 3. (b) Corresponding translocation frequency against voltage for four selected lengths. Error bars are from the standard errors of the Gaussian fits to the ECD histogram.

are from a least-squares fit to the data in Fig. 4a using the model given by equation (1) and Fig. 3. Three parameters; i) the diffusion coefficient divided by pore length, ii) effective DNA charge and iii) entropic barrier height were globally fitted to the data set and converge with an entropic barrier height $u_0 = 4 kT$. Comparison of the data and fit in Fig. 4a shows that the fit deviates for long lengths at low voltage and for short lengths at high voltage. However, the model accurately captures the trend of increasing translocation frequency with length and the changing gradient with voltage.

Fig. 4b shows the same data as Fig. 4a plotted as translocation frequency against voltage for four selected lengths. For 0.5 kbp, 2 kbp and 3 kbp the translocation frequency is an increasing non-linear function in voltage and for 8 kbp it is unclear whether the translocation frequency increases linearly or slightly non-linearly over the voltage range. The model fits show a non-linear increase for 0.5 kbp, 2 kbp and 3 kbp in agreement with the data and for 8 kbp show a transition from non-linear to linear though this transition is not clearly observable in the data due to the larger error bars for 8 kbp.

In general the model predicts two regimes of (1) entropic barrier dominated and (2) drift dominated transport [19]. The entropic barrier regime dominates for low voltages and small dsDNA lengths and is characterised by a non-linear increasing translocation frequency

with voltage and increasing translocation frequency with length. The drift regime occurs at high voltage and for long dsDNA lengths where equation (1) reduces to give a translocation frequency

$$\frac{J(L)}{c_0} = \frac{\mu V_m}{L}, \quad (2)$$

where V_m is the applied voltage and therefore the translocation frequency is linear in voltage and independent of dsDNA length. The results presented here in 4M LiCl show the characteristics of the entropic barrier regime. At higher voltages in Fig. 4a it can be seen that the translocation frequency is only slightly increasing with length for the longer lengths and this together with the close to linear translocation frequency for 8 kbp in Fig. 4b suggests that the longer DNA lengths and higher voltage are on the threshold of the drift-dominated regime.

The transition point between barrier-limited and drift-dominated regimes is expected to be sensitive to a number of experimental factors namely pore size and geometry, DNA effective charge (via the type of salt and the salt concentration) and temperature. The 4M LiCl electrolyte reduces DNA velocity 10 times compared to 1M KCl (a commonly used electrolyte for nanopores) which can be related to a 10 fold decrease in the effective DNA charge [26]. We also performed experiments using 1M KCl as the electrolyte where the experimental resolution is limited to 5 kbp due to the faster translocation speed (Fig. 5a). A linear voltage dependence of translocation frequency is observed for 5 kbp, 10 kbp and 20 kbp DNA with no significant difference between the translocation frequency for these three lengths indicating a drift-dominated behaviour in this length regime and salt concentration (Fig. 5b). The lack of a significant barrier for translocation can also be observed by extrapolating the straight line fit to the data which shows that it intercepts close to the origin. Our results therefore show that the threshold voltage for drift-dominated transport is significantly decreased in 1M KCl compared to 4M LiCl due to the higher effective charge.

To conclude, we have investigated the translocation frequency of dsDNA through quartz nanopores with mean diameter 15 nm. The low noise of these nanopores, combined with the narrow distribution of dwell times for individual lengths in such wide pores, allows us to accurately measure the translocation frequency using calibrated DNA samples. Using an electrolyte of 4M LiCl we have observed an increasing translocation frequency as a function of DNA length in the range 0.5 kbp to 10 kbp which fits the behaviour of entropic barrier-limited transport in a 1D convection-diffusion equation and allows us to extract an approximate value of 4 kT for the entropic barrier in this model. At a lower salt concentration of 1M KCl where the effective DNA charge is higher, we measure the characteristic transport properties of a drift-dominated regime. Our model accounts for the behaviour in these two different regimes and pro-

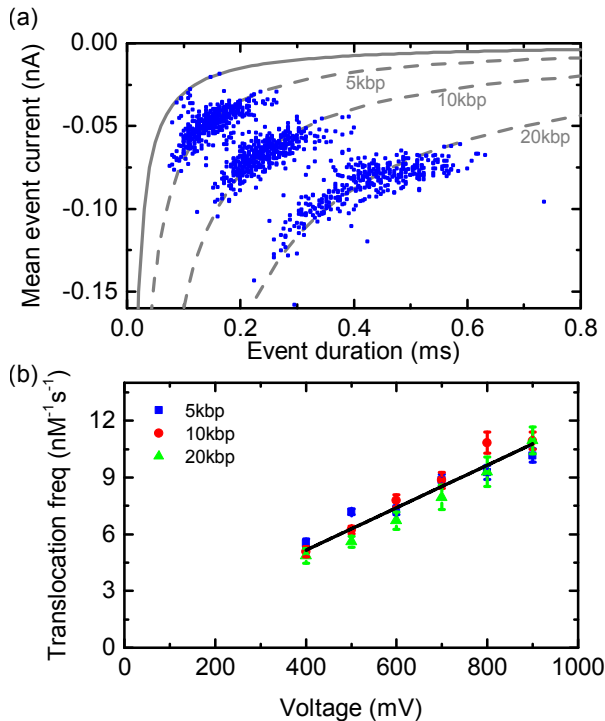


FIG. 5. (a) Scatter plot of 1168 translocations from a sample containing 5 kbp, 10 kbp and 20 kbp with each length at a concentration of 0.12 nM and using 1M KCl electrolyte with +600 mV applied voltage. The dashed grey lines are fits according to $\Delta I_{Mean} = -\frac{ECD_{Peak}}{\Delta t}$ and the solid line shows the 3 fC threshold. (b) Corresponding translocation frequency against voltage for 5 kbp, 10 kbp and 20 kbp - the translocation frequency values are significantly higher than that observed in 4M LiCl (Fig. 4b) due to the higher effective DNA charge in 1M KCl. The line shows a linear fit to all data points yielding a gradient of $0.011 \text{ nM}^{-1} \text{ s}^{-1} \text{ mV}^{-1}$. Error bars are from the standard errors of the Gaussian fits to the ECD histogram.

vides a basis for understanding and predicting polymer transport through nanopores across a wide range of conditions.

We thank Nadanai Laohakunakorn for finite element analysis calculations and useful discussions. NAWB was supported by an EPSRC doctoral prize and an ERC starting grant (Passmembrane 261101), UFK acknowledges support from an ERC starting grant (Passmembrane 261101). MM acknowledges grants from the National Institutes of Health (Grant No. R01HG002776-11) and AFOSR (Grant No. FA9550-14-1-0164) and support

from a Royal Society travel grant.

- [1] D. Branton, D. W. Deamer, A. Marziali, H. Bayley, S. A. Benner, T. Butler, M. Di Ventra, S. Garaj, A. Hibbs, X. Huang, et al., *Nat. Biotechnol.* **26**, 1146 (2008).
- [2] M. Muthukumar, *Polymer Translocation* (CRC Press, 2009).
- [3] S. E. Henrickson, M. Misakian, B. Robertson, and J. J. Kasianowicz, *Phys. Rev. Lett.* **85**, 3057 (2000).
- [4] A. Meller and D. Branton, *Electrophoresis* **23**, 2583 (2002).
- [5] T. Ambjornsson, S. P. Apell, Z. Konkoli, E. A. Di Marzio, and J. J. Kasianowicz, *J. Chem. Phys.* **117**, 4063 (2002).
- [6] M. Wanunu, W. Morrison, Y. Rabin, A. Y. Grosberg, and A. Meller, *Nat. Nanotechnol.* **5**, 160 (2010).
- [7] A. Y. Grosberg and Y. Rabin, *J. Chem. Phys.* **133**, 165102 (2010).
- [8] M. Wanunu, J. Sutin, B. McNally, A. Chow, and A. Meller, *Biophys. J.* **95**, 4716 (2008).
- [9] M. van den Hout, V. Krudde, X. J. A. Janssen, and N. H. Dekker, *Biophys. J.* **99**, 3840 (2010).
- [10] S. Ghosal, *Phys. Rev. E* **74**, 041901 (2006).
- [11] S. Ghosal, *Phys. Rev. Lett.* **98**, 238104 (2007), 0709.3850.
- [12] M. Mihovilovic, N. Hagerty, and D. Stein, *Phys. Rev. Lett.* **110**, 028102 (2013).
- [13] A. Storm, J. Chen, H. Zandbergen, and C. Dekker, *Phys. Rev. E* **71**, 051903 (2005).
- [14] J. Li, M. Gershow, D. Stein, E. Brandin, and J. A. Golovchenko, *Nat. Mater.* **2**, 611 (2003).
- [15] N. A. W. Bell and U. F. Keyser, *J. Am. Chem. Soc.* **137**, 2035 (2015).
- [16] L. J. Steinbock, O. Otto, C. Chimere, J. Gornall, and U. F. Keyser, *Nano Lett.* **10**, 2493 (2010).
- [17] C. S. Lengsfeld and T. J. Anchordoquy, *J. Pharm. Sci.* **91**, 1581 (2002).
- [18] J. J. Kasianowicz, E. Brandin, D. Branton, and D. W. Deamer, *P. Natl. Acad. Sci. USA* **93**, 13770 (1996).
- [19] M. Muthukumar, *J. Chem. Phys.* **132**, 195101 (2010).
- [20] N. Laohakunakorn, S. Ghosal, O. Otto, K. Misiunas, and U. F. Keyser, *Nano Lett.* **13**, 2798 (2013).
- [21] N. Laohakunakorn, V. V. Thacker, M. Muthukumar, and U. F. Keyser, *Nano Lett.* **15**, 695 (2015).
- [22] R. Kumar and M. Muthukumar, *J. Chem. Phys.* **131**, 194903 (2009).
- [23] S. S. Sorlie and R. Pecora, *Macromolecules* **23**, 487 (1990).
- [24] R. M. Robertson, S. Laib, and D. E. Smith, *P. Natl. Acad. Sci. USA* **103**, 7310 (2006).
- [25] N. C. Stellwagen, C. Gelfi, and P. G. Righetti, *Biopolymers* **42**, 687 (1997).
- [26] S. W. Kowalczyk, D. B. Wells, A. Aksimentiev, and C. Dekker, *Nano Lett.* **12**, 1038 (2012).